

# Electrical conductivity studies of sodium borate system based on diffusion controlled relaxation model

R. MURUGARAJ, G. GOVINDARAJ\*, R. SUGANTHI, D. GEORGE  
*Raman School of Physics, Pondicherry University, Pondicherry 605 014, India*  
*E-mail: ggraj\_54@mailcity.com; purm72@mailcity.com*

A.c. conductivity measurements and its analysis are performed on the  $x\text{Na}_2\text{O} + (1-x)\text{B}_2\text{O}_3$  ionic conducting glass system, where  $0.05 < x < 0.45$ . The a.c. conductivity data are analysed using both Jonscher's power law and diffusion controlled relaxation (DCR) model. The DCR model is used to interpret the observed dispersion in a.c. conductivity in terms of diffusion controlled dielectric loss relaxation mechanism. All the known experimental features of the  $\sigma'(\omega)$  including scaling behavior are explained satisfactorily. The results show an excellent agreement with scaling behavior based on loss peak frequency.

© 2003 Kluwer Academic Publishers

## 1. Introduction

The electrical conduction study on fast ion conducting glasses particularly play an important role and are often the deciding factors about the suitability of the material for a particular electrochemical device. The measured a.c. conductivity consists of intrinsic conductivity of materials along with electrode resistance and electrode sample interface resistance. Therefore, extraction of intrinsic conductivity is essential for a material. One of the most important characteristic properties of disordered solids is the strong dispersion of the real part of the a.c. conductivity [1–17]. At low frequencies one observes a constant conductivity, while at high frequencies, the conductivity becomes strongly frequency dependent, varying approximately as a fractional power of frequency. The increase in conductivity usually continues up to phonon's frequencies. In the literature, several theoretical models have been proposed to explain the observed dispersive behavior in a.c. conductivity [18–22]. In this context, the observed dispersive behavior in a.c. conductivity is discussed mainly in terms of dielectric loss relaxation processes or conductivity relaxation processes. In the present paper, we have studied the a.c. conductivity dispersion and its scaling behavior in  $x\text{Na}_2\text{O} + (1-x)\text{B}_2\text{O}_3$  glassy system as a function of compositions  $0.05 < x < 0.45$ . The observed a.c. conductivity dispersion is analysed with the dielectric loss relaxation process associated in the diffusion controlled relaxation model and Jonscher's universal power law.

## 2. Experimental procedure

Sodium carbonate and boric acid were taken as the ingredients for the preparation of  $x\text{Na}_2\text{O} + (1-x)\text{B}_2\text{O}_3$  ionic conducting glass system, where  $0.05 < x < 0.45$ . The raw materials were taken in open silica crucibles

melted in a furnace for 30 to 45 min at about 800–900°C (depending upon the composition). During the melting process, the crucible was shaken frequently to ensure the homogeneous mixing of all substances. The melt was poured between two stainless steel plates, which was kept at room temperature. The resulting glass samples were brittle. These glasses were pulverised into fine powder and pressed into pellets of 10 mm diameter and about 1 mm thick by applying a pressure of 5000–6000 kg/cm<sup>2</sup> for about 15 min using a hand press. The prepared samples of the  $x\text{Na}_2\text{O} + (1-x)\text{B}_2\text{O}_3$  system with  $x$  varying from 0.05 to 0.45 were subjected for the X-ray diffraction (XRD) studies. The peak less XRD patterns confirmed that the samples were amorphous in nature. In order to ascertain their glassy nature, they have been subjected to DSC studies. A.c. electrical measurements were carried out by sandwiching the pellets between electrical leads made of silver. Zentech 3305 component analyser (TAIWAN) was used to measure the capacitance  $C_p$  and conductance  $G_p$  in the frequency range 20 Hz to 1 MHz at different temperatures. Analysis was made by using impedance spectroscopy technique to extract the information about the bulk properties of the sample. Complex impedance analysis was carried out for the samples at different temperatures from the measured  $G_p$  and  $C_p$  values through the admittance  $Y^*$  of the sample:

$$Y^* = G_p + j\omega C_p = 1/Z^* \quad (1)$$

Fig. 1 shows the impedance dispersion for the sample  $0.4\text{Na}_2\text{O} + 0.6\text{B}_2\text{O}_3$  at 396 K. The impedance plot shows combined arcs of two different semi-circles. From the plot, one can see that the electrode sample interface dispersion is more pronounced at low frequency

\*Author to whom all correspondences should be addressed.

TABLE I The magnitude of Cole-Cole exponent  $\alpha$ , the mean relaxation time  $\tau_m$ , room temperature d.c. conductivity and  $\tau/\tau_1$  for the  $x\text{Na}_2\text{O} + (1-x)\text{B}_2\text{O}_3$  glass system

Composition $x$	$\sigma_{dc}$ (300 K) ( $\text{S m}^{-1}$ )	$\alpha$	$\tau_m$ (sec)	$n$	$\tau/\tau_1$
0.05	$1.352 \times 10^{-8}$	0.0642	$1.613 \times 10^{-3}$	0.9122	1.059
0.10	$5.121 \times 10^{-7}$	0.0438	$6.377 \times 10^{-3}$	0.9288	1.098
0.15	$6.464 \times 10^{-9}$	0.0209	$5.138 \times 10^{-3}$	0.9685	1.194
0.20	$1.954 \times 10^{-8}$	0.0514	$4.849 \times 10^{-3}$	0.9877	1.242
0.25	$5.205 \times 10^{-9}$	0.0574	$1.424 \times 10^{-3}$	0.9334	1.109
0.30	$3.045 \times 10^{-8}$	0.0105	$9.409 \times 10^{-5}$	0.8524	0.924
0.35	$9.824 \times 10^{-9}$	0.0031	$1.725 \times 10^{-3}$	0.9156	1.067
0.40	$1.673 \times 10^{-8}$	0.0281	$1.272 \times 10^{-3}$	0.9350	1.113
0.45	$1.399 \times 10^{-7}$	0.0752	$1.774 \times 10^{-4}$	0.9248	1.089

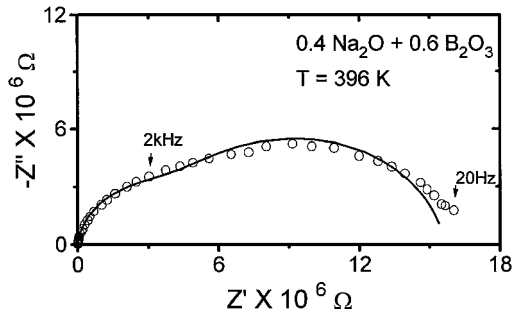


Figure 1 Impedance spectrum of the sample  $0.4\text{Na}_2\text{O} + 0.6\text{B}_2\text{O}_3$  at 396 K.

region, and in high frequency region the depressed semi-circle may be due to the dispersive behavior of the sample bulk resistance and the corresponding Cole-Cole type constant phase element (CPE),  $Q_o(j\omega)^{-(1-\alpha)}$  [23, 24]. The frequency dispersion based on the final parameter set is compared with the total measured dispersion in the fit quality plot using dispersion simulation program [25]. Similar procedure is followed to analyze the various compositions of the compounds at different temperatures. From Fig. 1, the high frequency depressed semi-circle do not pass through origin, because it satisfies the condition  $Z_\infty > 0$ . The depressed semi-circle below the real axis indicates that the relaxation time  $\tau$  is not single valued, but it is distributed continuously or discretely around the mean relaxation time  $\tau_m$ . The width of the distribution of relaxation time is related to the angle through which the semi-circle is depressed below the real axis or through the CPE exponent  $\alpha$ . The magnitude of the constant phase element exponent  $\alpha$  of the high frequency region for all the samples at room temperature is shown in Table I along with the mean relaxation time  $\tau_m$ .

The bulk d.c. resistances at different temperature for all the compositions are obtained from the analysis of impedance plane plots. The d.c. electrical conductivity of the sample is given by:

$$\sigma_{dc} = \frac{d}{Ra} \text{S m}^{-1}, \quad (2)$$

where  $d$  is the thickness of the pellet in metre;  $a$  is the area of cross section in  $\text{m}^2$  and  $R$  is the bulk resistance in ohms obtained from impedance plot. The values of room temperature d.c. conductivity are reported in Table I. The temperature dependence of d.c. conductivity in the form of  $\log(\sigma_{dc}T)$  versus  $1000/T$  was

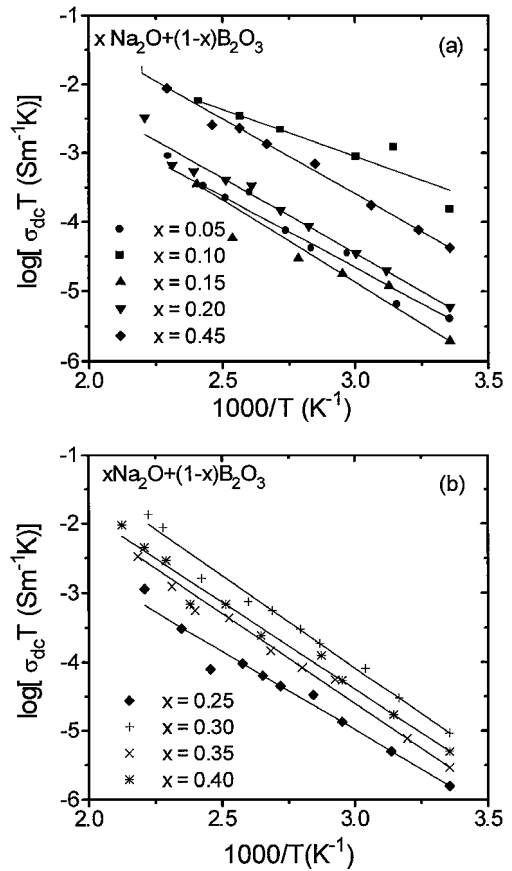


Figure 2 (a)  $\log[\sigma_{dc}T]$  versus  $1000/T$  of the prepared glass samples under investigation. (b)  $\log[\sigma_{dc}T]$  versus  $1000/T$  of the prepared glass samples under investigation.

plotted for all the compositions and results are shown in Fig. 2a and b. It is found that the d.c. conductivity increases with increasing temperature and obeys the Arrhenius equation

$$\sigma_{dc}T = \sigma_o e^{-E_{dc}/k_B T}. \quad (3)$$

The d.c. activation energy for the conduction is calculated from the slope of the  $\log(\sigma_{dc}T)$  versus  $1000/T$  for various compositions of the samples. Fig. 3 shows the variation of d.c. activation energy with different compositions of the prepared samples. The d.c. activation energy variation is found to be non-linear as the composition changes.

The measured conductance  $G_p(f)$  values were used to study the a.c. conductivity behavior of the prepared

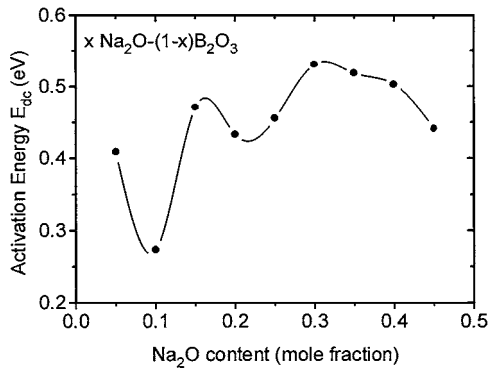


Figure 3 Variation of d.c. activation energy ( $E_{dc}$ ) as a function of  $\text{Na}_2\text{O}$  content.

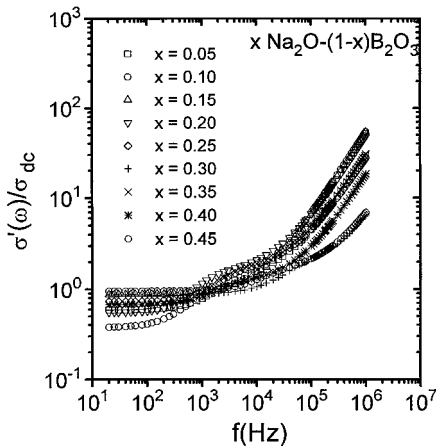


Figure 4  $\log[\sigma'(\omega)/\sigma_{dc}]$  as a function of  $\log[\text{frequency}]$  of the investigated samples at room temperature before suppressing the electrode-sample interface contribution.

samples. The a.c. conductivity exhibits dispersive behavior as a function of frequency  $f$ . Fig. 4 shows the a.c. conductivity behavior of the prepared samples scaled by the respective bulk d.c. conductivity at room temperature. The dispersion in low frequency region (upto 1 kHz) is due to the polarisation of the electrode sample interface effect. With equivalent circuit analysis, the dispersion due to electrode-sample interface effect is suppressed and the real part of the conductivity is calculated for further analysis, which is dealt in the Section 4. The knowledge of conductivity behavior is therefore often used to infer information concerning about dynamic behavior of ions in the materials. Even then, a proper understanding of the a.c. conduction is important in order to arrive at a correct picture of d.c. transport. The simplest and indeed the most common explanation for increase of conductivity with frequencies is the existence of one or other kind of inhomogeneities present in the solid. The inhomogeneities may be of a microscopic or a macroscopic nature, a question, which is not yet settled. In the next section, a review on models of a.c. conduction with brief discussion on the diffusion controlled relaxation model for ionic transport in fast ionic conductors will be presented.

### 3. Models in disordered ionic conductors-DCR model

Measurement of impedance or conductivity alone are usually not enough, however, much more can be learned when the measured data are interpreted using appro-

priate models and its corresponding equations. Present section is the discussion on Jonscher's empirical equations [18, 19, 26], which have proved useful for a.c. conductivity data analysis and a plausible physically realistic model, namely diffusion controlled relaxation model [27–30].

In many non-metallic ionic conductors d.c. or a.c. electrical conductivity is the result of diffusion of ions through the ionic conductors. Almond and others [31–33] pointed out, that the dispersive behavior of a.c. conductivity of disordered solids, which have ionic conducting nature can be expressed in the form [18, 19];

$$\sigma'(\omega) = \sigma(o) + A\omega^n, \quad o < n < 1. \quad (4)$$

It should be note that the total measured a.c. conductivity in the additive form characterised by Equation 4 actually implies that the a.c. and d.c. conductivities are independent and that they arise from different mechanisms. On the other hand, the d.c. conductivity is the zero frequency limit of the a.c. conductivity, i.e.,  $\sigma(o) = \sigma'(\omega \rightarrow o)$ , means that only a single mechanism is involved in the conductive response. As a common feature, it has been postulated that the observed dynamic conductivity dispersion is also due to the polarisation loss mechanism by ions diffusion through the solid. In general, both conductivity and dipolar relaxation process may be present in the same material, then the total conductivity is given by,

$$\sigma^*(\omega) = \sigma(o) + j\omega\varepsilon_0\varepsilon^*(\omega), \quad (5)$$

where  $\sigma(o)$  is the long range or frequency independent or d.c. conductivity;  $\varepsilon_0$  is the permittivity of the free space and  $\varepsilon^*(\omega)$  is the complex dielectric constant defined by  $\varepsilon^*(\omega) = \varepsilon'(\omega) - j\varepsilon''(\omega)$ , where  $\varepsilon'(\omega)$  and  $\varepsilon''(\omega)$  are the real and imaginary parts of the complex dielectric constant. Therefore, the real part of the a.c. conductivity is given by

$$\sigma'(\omega) = \sigma(o) + \omega\varepsilon_0\varepsilon''(\omega). \quad (6)$$

Jonscher has stated that  $\varepsilon''(\omega)$  is proportional to the combination of two terms with respect to dielectric loss peak frequency and it is given by

$$\varepsilon''(\omega) \propto [(\omega/\omega_p)^{-m} + (\omega/\omega_p)^{(1-n)}]^{-1}, \quad (7)$$

where the first term corresponds to  $\omega < \omega_p$  and the second term corresponds to  $\omega > \omega_p$ . The exponents  $m$  and  $n$  are arbitrary parameters and both are smaller than unity. The Jonscher's universal power law Equation 4 is obtained from Equation 7 by means of identification of  $m = -1$  [31–33]. Thus the a.c. conductivity becomes

$$\sigma'(\omega) = K\omega_p + K\omega_p^{(1-n)}\omega^n \quad (8)$$

where  $K$  is constant and contains the information about the carrier concentration, ion hopping distance, etc. Comparing Equation 8 and Equation 4, one finds that

$\sigma(\omega) = K \omega_p$  and  $A = \sigma(\omega)/\omega_p^n$ . The first term is the frequency independent d.c. conductivity and the second term is the dispersive component of conductivity in a characteristic power law with exponent  $n$ .

There are two basic types of theory that have been used to describe the observed dispersive behavior of electrical properties in disordered ionic conductors. In the first, the high frequency power law is assumed to represent the high frequency part of a relaxation process whose low frequency part is covered by d.c. conductivity. This relaxation process is assumed to be result from hopping of ions over local energy barriers at high frequencies. The second view interprets that the frequency dependence of the conductivity is the result of changes in the diffusion of mobile ion. At low frequencies, the mean square displacement of diffusing ions is linear in time which results a constant coefficient of diffusion and hence d.c. conductivity. At high frequencies the ion is influenced by the interactions with nearest neighboring ions, exhibits a dispersive behavior in mean square displaced and hence the dispersive conductivity.

In the literature, the a.c. conductivity in disordered solids assumes that a broad frequency response from relaxation of a number of sites, acting independently with a distribution of relaxation times. However, in contrast with the distribution of the relaxation times, there is an alternative picture in which the electrically relaxing centres are strongly coupled with each other and with the result of the relaxation process occurs in series, each site constraining the relaxation of the others through the stretched exponential relaxation function [34, 35].

$$\phi(t) = e^{-(t/\tau)^{\beta_{sw}}} \quad (9)$$

It is clear from Equation 9, that the time dependent relaxation of the dielectric polarisation after the application of an electric field is not simple exponential.

The DCR model appears to be the simplest available model, which can satisfactorily account for a wide variety of experimental data with the minimum assumptions. The relaxation process in the absence of interaction by other ions are described through Debye relaxation process for the diffusing ions and it is given by

$$\phi(t) = e^{-(t/\tau)}, \quad (10)$$

where  $\tau$  is the relaxation time. The complex permittivity  $\varepsilon^*(\omega)$  or the complex susceptibility  $\chi^*(\omega) = \varepsilon^*(\omega) - 1$  is obtained by taking imaginary Laplace transform of the derivative of the relaxation function,

$$L \left[ -\frac{d\phi}{dt} \right] = L \left[ \frac{1}{\tau} e^{-t/\tau} \right] = \frac{\varepsilon^*(\omega) - \varepsilon_\infty}{\varepsilon_s - \varepsilon_\infty}, \quad (11)$$

where  $\varepsilon_s$  and  $\varepsilon_\infty$  are the static or d.c. and high frequency limits of the permittivity and  $L[\ ]$  is the imaginary Laplace transform operator. By using Equation 6, the real part of the conductivity is given by

$$\sigma'(\omega) = \sigma(\omega) + \frac{\varepsilon_0(\varepsilon_s - \varepsilon_\infty)\omega^2\tau}{1 + \omega^2\tau^2}. \quad (12)$$

In the high frequency region i.e.,  $\omega\tau \gg 1$ , the real part of the conductivity is independent of frequency. However, the literature shows that the real part of the conductivity obeys power law frequency dependence at sufficiently high frequencies. The exponent  $n$  in the power law frequency dependence is increasing with decreasing temperature. Further, the peak in dielectric loss, which is often asymmetric and much broader than that expected for a Debye loss peak.

The DCR model is proposed to explain the microscopic transport mechanism of ion conducting glasses. The DCR model is applicable in the presence of non-bridging oxygen (NBO) sites in the ionic material. Ion transport occurs by means of diffusive motion between the cation interstitial sites consisting of many equivalents position around each NBO site. In DCR model, the dielectric polarisation occurs principally by means of an interstitially like mechanism, in which an ion diffuse to a site and cause the ion already residing at the site to move to another equilibrium position via mutual Coulomb repulsion. The time scale in this case is stretched by the diffusion time between two sites. Therefore, the temporal response function is defined as:

$$\phi(t) = e^{-(t/\tau)}(1 - P(t)). \quad (13)$$

The first term is the diffusion independent relaxation involving the relaxation time  $\tau$ . The second term involves the instantaneous relaxation caused by the arrival of a second ion to form an interstitial pair. Diffusion independent relaxation can occur at a given site by the thermally activated motion. This is the origin of the  $\exp(-t/\tau)$  term in Equation 13, where  $P(t)$  is the time dependent probability of trigger ion which has reached the new site from original site by the time  $t$ . The factor  $(1 - P(t))$  is the probability that such an ion has not yet arrived and it is defined as for one dimension:

$$1 - P(t) = e^{-\frac{2Dt/\pi}{l_0}}, \quad (14)$$

where  $D$  is the diffusion constant of the defect and  $1/2 l_0$  is the average number of triggering ions or defects per unit length. On substituting Equation 14 in Equation 13,

$$\phi(t) = e^{-(t/\tau)} e^{-(t/\tau_1)^{1/2}}, \quad (15)$$

where  $\tau_1 = \pi l_0^2 / 4D$  and when  $\tau_1 \rightarrow \infty$  then the relaxation process is a Debye type. If  $\tau/\tau_1 > 1$  and  $\tau/\tau_1 < 1$  the relaxation process is of Cole-Cole type [23] and Cole Davidson type [36] respectively. The dielectric permittivity of DCR model is obtained by using Equation 15 with Equation 11. In this case, the diffusion triggered relaxation and diffusion independent relaxation together are responsible for frequency dependent behavior of  $\sigma'(\omega)$ . Thus, in DCR model, one can distinguish two types of ionic motion, which give rise to qualitatively different behavior. At first, a steady diffusive motion of ions occur through the material under the action of an applied electric field, accompanied by a polarisation relaxation at each intervening NBO site

involved. Thus, this mechanism gives rise to a combination of a.c. and d.c. conductivities.

By Equations 6, 11 and 15, one can observe that the dispersion in  $\sigma'(\omega)$  through the diffusion independent relaxation  $\tau$  and diffusion triggered relaxation  $\tau_1$ . In the next section, the observed results of  $\sigma'(\omega)$  are analysed using both Jonscher's UPL through the frequency exponent  $n$  and DCR model through  $\tau/\tau_1$  ratio.

## 4. Results and discussion

### 4.1. A.C. conductivity analysis

The measurement of small signal a.c. frequency response of ionic conducting materials over a wide range of frequencies, i.e., impedance spectroscopy, is becoming a valuable tool with the advent of automatic component analysing equipment. The starting point in the conductivity data analysis is the conversion of experimentally measured impedance into admittance with proper suppression of electrode resistance, electrode-sample interface resistance and electrode sample interface constant phase element.

The complex plane plots of the prepared samples at different temperatures have broad asymmetric arcs similar to Fig. 1. In the present work, the equivalent circuit representation is used to analyse the bulk property of the sample and interface responses. The electrode sample interface resistance and interface CPE responses are suppressed in the impedance representation at all frequencies. The sample a.c. response alone is identified for further studies. The sample response, the real part of a.c. conductivity scaled by d.c. conductivity as a function of frequency is shown in Fig. 5 for different compositions at room temperature.

The conductivity spectra show a constant conductivity at low frequencies while at high frequencies, the conductivity becomes strongly frequency dependent, varying approximately power of the frequency. Frequency exponent  $n$  in Equation 4 is calculated using non-linear least square fit procedure of Levenberg-Marquardt [37]. In Fig. 5, the values of  $n$  are shown between two brackets. The  $n$  values are less than unity and have the same variation of the constant phase element exponent  $(1 - \alpha)$  of the sample contribution.

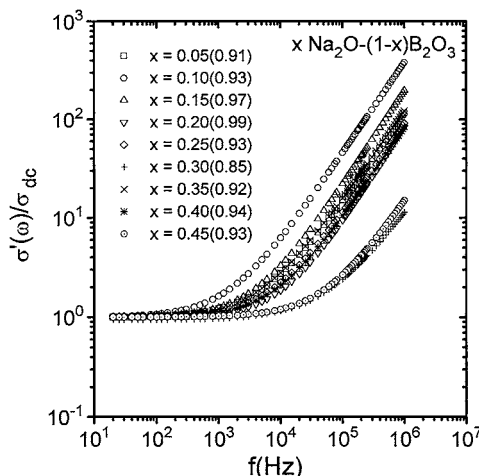


Figure 5  $\log[\sigma'(\omega)/\sigma_{dc}]$  as a function of  $\log[\text{frequency}]$  of the investigated samples at room temperature after suppressing the electrode-sample interface contribution.

The principal result of DCR model is, that the dispersion in  $\sigma'(\omega)$  or  $\varepsilon''(\omega)$  is dealt through  $\tau$  and  $\tau_1$  with the assumption that, the dielectric loss relaxation process is the same as that of Jonscher's dielectric loss  $\varepsilon''(\omega)$ . It is possible to write the exponent  $n$  as [27–30]

$$n = [\pi\tau/4\tau_1]^{1/2}. \quad (16)$$

Using fitted values of  $n$  from Equation 4, the values of  $\tau/\tau_1$  are calculated using Equation 16. In Table I, the values of  $\tau/\tau_1$  are reported as a function of composition at room temperature. It is observed that the magnitude of  $\tau/\tau_1$  greater than one except for the sample  $x = 0.3$ . According to DCR model,  $\tau/\tau_1 > 1$ , corresponds to Cole-Cole type dispersion. The dispersion in  $\sigma'(\omega)$  through DCR model and Jonscher's universal law analysis shows that the origin of dispersion is CPE present in the sample and it is of Cole-Cole type.

### 4.2. Scaling behavior in a.c. conductivity

The scaling and universality features are seen prominently by the ion relaxation mechanisms in disordered solids. Recently, there has been renewed interest in the scaling and the striking similarity of a.c. conduction in quite different solids [1, 3, 7, 38, 39]. It is usually possible to scale the temperature and composition dependence of conductivity spectra into a single master curve. In the literature, the scaling behavior in a.c. conductivity is studied using either with loss peak frequency or with  $\omega_c$  which is characteristic, but arbitrary determined frequency. Sidebottom in his recent work [5], suggested a universal approach for scaling the a.c. conductivity by defining, the dielectric loss strength. Some disordered solids do not possess well defined dielectric loss peaks, and as a consequence the value of the static dielectric constant or dielectric loss strength could not be obtained from the frequency dispersion dielectric data. Under these circumstances, the frequency axis is scaled with respect to hopping frequency which automatically taken into account the dielectric loss strength and correlation effects during diffusion of ions in disordered lattice [7]. Therefore, we use Jonscher's loss peak frequency as scaling frequency for the frequency axis.

The loss peak frequency is calculated using Equation 4 with  $A = \sigma(o)/\omega_p^n$  defined by Almond and West [27–29]. Then the Equation 4 becomes,

$$\sigma(\omega) = \sigma(o) + \sigma(o)\omega^n/\omega_p^n \quad (17)$$

By using fitted values of  $A$ ,  $n$  and d.c. conductivity, the value of  $\omega_p$  is calculated. The variation of  $\omega_p$  as a function of composition at room temperature is shown in Fig. 6. The real part of a.c. conductivity for different compositions at room temperature are scaled by the respective d.c. conductivity and plotted as a function of  $\omega/\omega_p$  and are shown in Fig. 7. From this figure, it is evident that all the dispersive curves collapse on a single master curve. Therefore, the frequency scaling by  $\omega_p$  on the frequency axis shows universal dispersive behavior of a.c. conductivity.

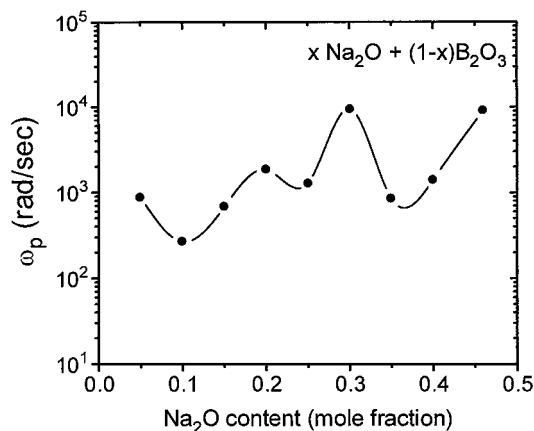


Figure 6 Composition dependence of loss peak frequency  $\omega_p$  at room temperature of the investigated samples.

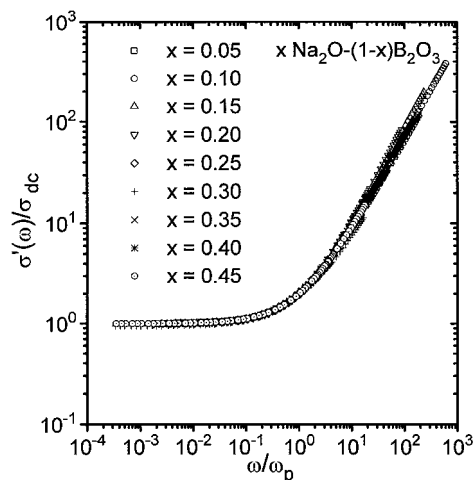


Figure 7  $\sigma'(\omega)/\sigma_{dc}$  as function of  $\omega/\omega_p$  of the investigated samples at room temperature.

## 5. Conclusion

In the present work, the electrical properties of various composition of sodium borate glasses at different temperatures are studied. The measured a.c. data are analysed using the diffusion controlled relaxation mechanism and Jonscher universal power law to explain the observed dispersive behavior of the electrical conductivity. Using impedance spectroscopy technique, the data are analysed based on Cole-Cole type impedance response function. The values of frequency exponent  $n$  of Jonscher's universal power law of a.c. conductivity as a function of the samples composition at room temperature are calculated. The DCR model is used to explain the observed dispersive behavior of a.c. conductivity through the diffusion triggered relaxation and diffusion-independent relaxation times. The scaling behavior in a.c. conductivity is satisfactorily explained by scaling the frequency axis by loss peak frequency.

## Acknowledgements

This work is supported under financial assistance of UGC research award scheme 30-64/98/SA-II. One of the authors (RM) is thankful to UGC, Govt. of India for SRF assistance.

## References

1. J. C. DYRE and T. B. SCHRÖDER, *Rev. of Mod. Phys.* **72** (2000) 873.
2. K. L. NGAI and C. LEON, *Phys. Rev. B* **60** (1999) 9396.
3. T. B. SCHRÖDER and J. C. DYRE, *Phys. Rev. Letts.* **84** (2000) 310.
4. D. L. SIDDEBOTTOM, P. F. GREEN and R. K. BROW, *Phys. Rev. Letts.* **74** (1995) 5068.
5. D. L. SIDDEBOTTOM, *ibid.* **82** (1999) 3653.
6. J. C. DYRE, *Phys. Rev. B* **49** (1994) 11709; *Idem., ibid.* **B 50** (1994) 9692.
7. A. GHOSH and A. PAN, *Phys. Rev. Letts.* **84** (2000) 2188.
8. A. E. OWEN, *J. Non-Cryst. Solids* **25** (1977) 370.
9. B. ROLING, *Solid State Ionics* **105** (1998) 185.
10. S. R. ELLIOT, **70/71** (1994) 27.
11. H. KAHNT and BER. BUNSENGES, *Phys. Chem.* **95** (1991) 1021.
12. B. K. KUANG and G. P. SRIVASTAVA, *J. Appl. Phys.* **75** (1994) 6115.
13. M. M. JASTRZEBSKA, S. JUSSILA and H. ISOTALO, *J. Mater. Sci.* **33** (1998) 4023.
14. S. A. ROZANSKI, F. KREMER, P. KOBERLE and A. LASCHEWSKY, *Macromol. Chem. Phys.* **196** (1995) 877.
15. M. SUZUKI, *J. Phys. Chem. Solids* **41** (1980) 1253.
16. R. F. BIANCHI, P. H. SOUZA, T. J. BONAGAMBA, H. C. PANEPUCCI and R. M. FARIA, *Synth. Met.* **102** (1999) 1186.
17. C. A. ANGELL, *Chem. Rev.* **90** (1990) 523.
18. A. K. JONSCHER, *Nature (London)* **267** (1977) 673.
19. *Idem.*, "Dielectric Relaxation in Solids" (Chelsa Dielectric Press, London, 1983) p. 89.
20. S. R. ELLIOT, *Solid State Ionics* **27** (1988) 131.
21. J. C. DYRE, *J. Non-Cryst. Solids* **135** (1991) 219.
22. K. FUNKE, *Prog. Solid State Chem.* **22** (1993) 111.
23. K. S. COLE and R. H. COLE, *J. Chem. Phys.* **9** (1941) 341.
24. J. ROSS MACDONALD (ed.), "Impedance Spectroscopy" (John Wiley & Sons, New York, 1987) p. 17.
25. B. A. BOUKAMP, Equivalent Circuit Version 3.97 (Department of Chemical Tech., University of Twente, 7500, AE Enschede, The Netherlands, 1989).
26. A. K. JONSCHER, *Nature (London)*, **250** (1974) 191; *Idem., ibid.* **256** (1975) 556; *Idem., ibid.* **253** (1975) 717.
27. S. R. ELLIOT, *J. Non-Cryst. Solids* **166** (1993) 29.
28. *Idem.*, "Physics of Amorphous Materials" 2nd ed. (Longman Scientific & Technical, England, 1990) p. 255.
29. F. HENN, S. R. ELLIOT and J. C. GIUNTINI, *J. Non-Cryst. Solids* **136** (1991) 60.
30. S. R. ELLIOT and A. P. OWENS, *Phil. Mag. B* **60** (1989) 777.
31. D. P. ALMOND, G. K. DUNKAN and A. R. WEST, *Solid State Ionics* **8** (1983) 159.
32. D. P. ALMOND and A. R. WEST, *ibid.* **9/10** (1983) 277.
33. *Idem., ibid.* **23** (1987) 323.
34. G. GOVINDARAJ and R. MURUGARAJ, *Mater. Sci. Engg. B* **77** (2000) 60.
35. G. WILLIAMS and D. C. WATTS, *Trans. Faraday Soc.* **66** (1970) 80.
36. D. W. DAVIDSON and R. H. COLE, *J. Chem. Phys.* **19** (1951) 1484.
37. W. H. PRESS, S. A. TEUKOLSKY, W. T. VELLERLING and B. P. FLANNERY, "Numerical Recipes in Fortran" (Cambridge Univ. Press, 1996) p. 678.
38. D. L. SIDDEBOTTOM and J. ZHANG, *Phys. Rev. B* **62** (2000) 5503.
39. B. ROLING and C. MARTINY, *Phys. Rev. Letts.* **85** (2000) 1274.

Received 30 July 2001

and accepted 15 May 2002